ISSN: 2710-0588

# Study on Splitting Intensity and Acoustic Emission Characteristics of Brazilian Deep Gray Sandstone at Different Scales

Yiwen Zhang

School of Civil Engineering, Henan Polytechnic University, Jiaozuo, China

## Abstract

**In order to determine the influence of size on the mechanical properties of sandstone and acoustic emission damage characteristics, the Brazilian splitting test of 6 sandstone samples with diameters of 25mm, 37mm, 50mm, 69mm, 80mm and 100mm was carried out by using the rock weak surface direct shear instrument and acoustic emission monitoring system The effects of size change on the splitting strength, deformation, acoustic emission activity and damage characteristics of rock samples are discussed. The results show that the larger the specimen size is, the more original defects are contained in the specimen, which has a great influence on the development trend of stress-strain curve, peak strength and peak strain during loading. With the increase of sample size, the peak strength and peak strain become smaller and smaller, and the ratio of peak compressive strain to peak tensile strain remains in the range of 2~4 times. According to the development characteristics of acoustic emission signals, the whole process of rock damage is divided into four stages: micro-crack compaction stage, new crack generation and expansion stage, crack rapid expansion stage and failure stage. The diameter sample of 69mm~100mm showed almost no AE signal at the beginning of test loading, and the activity of acoustic emission signal is intense at the moment of failure.The larger the specimen size, the larger the stress value and b value corresponding to the fracture entering the instability expansion stage. Tensile microcracks are the main types of cracks in the splitting test, and with the increase of the size, the shear microcracks gradually decrease, and the tensile microcracks increase.**

## Keywords

**Sandstone; Size change; Mechanical properties; Acoustic emission.**

## 1. Introduction

Rock belongs to the natural brittle geological materials, its internal contains a large number of ore impurities, primary fissure, joints, etc., the native defect distribution position random, makes the rock material has complex size effect, namely the form, quantity, distribution location is different, lead to the differences in the internal mechanical properties. Due to the complexity of in situ test, the rock mechanics test in the laboratory is still the basis for rock mass engineering activities. However, due to the large difference between the two scales, attention must be paid to the impact of size effect. In view of this, multi-scale small size test is carried out indoors to master the mechanical properties of rock size effect. Through formula conversion and applied to engineering practice, it can avoid the occurrence of engineering accidents into some extent [1].

Many scholars for the size effect of experimental research and theory exploration, and achieved fruitful research results, among them, Zhang Sheng [2-4] analyzed the size change of sandstone dynamic compressive strength, fracture toughness test value, including the influence of crack time, put forward the method of dynamic fracture toughness. Zhao Guangming et al[5-6] believed that the elastic modulus and damage degree of the sample were positively correlated with the

ISSN: 2710-0588

high diameter ratio, and negatively correlated with the peak strain. Sun Hao et al. [7] studied the effect of temperature and size on the sandstone splitting strength, and believed that the effect of size is more obvious. Zhao Fei et al.[8] believes that the sample height is inversely proportional to the peak intensity and the acoustic emission energy rate. Liu Gang [9] analyzed the relationship between the sample size and the total AE energy and the count peak interval. Liu Hui [10] studied the effect of the freeze-thaw cycle number on the AE b value.Wang Yunfei et al [11] pointed out that the loading rate was positively correlated with the percentage of tensile cracks produced by sandstone failure, and the full water weakened this phenomenon.

The above research has achieved fruitful results, but the research content mainly focuses on the analysis of high diameter ratio and thickness ratio on rock strength, and few studies on the deformation characteristics and acoustic emission damage evolution characteristics of different sizes. In this paper, this paper discusses the characteristics of Brazilian splitting mechanics of different sizes, and describes the relationship between acoustic emission characteristic parameters and the size of the instability expansion and final failure of the internal fracture of different sizes, which provides a reference for the early warning of multi-scale rock mass in practical engineering.

## 2. The Brazilian Cleavage Test for The Sample Size Effect

### 2.1. Test instrument

KYZW-100 and DS2 Aemission signal analyzer were used as Brazilian split loading test and Aemission monitoring system, respectively. The maximum normal load of the direct shear instrument is 1000 KN, the maximum range of the normal displacement sensor is 300mm, and the measurement accuracy is 0.001mm. Radial displacement was recorded using two high sensitivity displacement sensors with a measurement accuracy of 0.001mm. The acquisition threshold for the acoustic emission instrument was set to 20 db with a sampling frequency of 3 MHz.

### 2.2. Experiment scheme

The test used 6 samples of 25mm thickness and diameter of 25,37,50,69,80, and 100mm. Three samples were selected for parallel testing. A speed of 0.001 mm/s was used to ensure the stability of the pressure head contact sample, the sample was prepressed at 0.2 KN for 60 seconds.

## 3. Analysis of the Test Results

### 3.1. Cleavage principle

For the Brazilian splitting test, the maximum tensile stress and the sample diameter where the loading path coincides, where the tensile stress maintains a certain magnitude.

The split strength is calculated as follows[12]:

$$\sigma_t = \frac{2P_{\max}}{\pi DL} \tag{1}$$

In the above formula,$\sigma_t$ is the tensile strength (MPa); $P_{max}$ is the maximum damage load (N); $D$ is the diameter of disc samples(mm); $L$ is the thickness of disc samples (mm).

Theoretically, the first cracking position of the sample is in the center, the compressive stress value at the crack is more than 3 times of the tensile stress, and the compressive strength is generally 8~10 times of the tensile strength. The damage of the specimen is identified as tensile damage [13]. The peak load is introduced into the formula (1) to obtain the tensile strength.

ISSN: 2710-0588

## 3.2. Analysis of intensity characteristics

Due to the brittleness and appearance characteristics of the disk sample itself, the stress is suddenly dropped after reaching the peak. The stress-strain curve of the disk sample with the same thickness and different diameters is shown in Figure 3. D indicates the diameter, the diameter of the first number indicates the diameter of the sample, and the last number indicates the serial number of the sample. It should be pointed out that: except for the tensile stress on the loading path is the same, the stress of the other points is not uniform, belonging to the non-uniform force. As can be seen from Figure 3, in the initial stage of loading, the tensile stress-pressure strain curve shows the concave state, which is due to the gradual closure of the internal pores of the sample under the action of lower load. The curve in this stage is called the compaction stage. The whole process curve of tensile stress-compression strain under the greater the splitting strength, the more obvious the sample shows the compaction process. According to the characteristics of the whole process curve of tensile stress-strain, the tensile stress-strain curve of each diameter sample is roughly divided into compaction stage-elastic stage-damage stage, and the tensile stress-strain curve is divided into elastic stage-destructive stage. With the increase of load, the strain and stress show a linear growth trend, reaching the peak load, the sample appears macroscopic crack, and then the damage occurs.

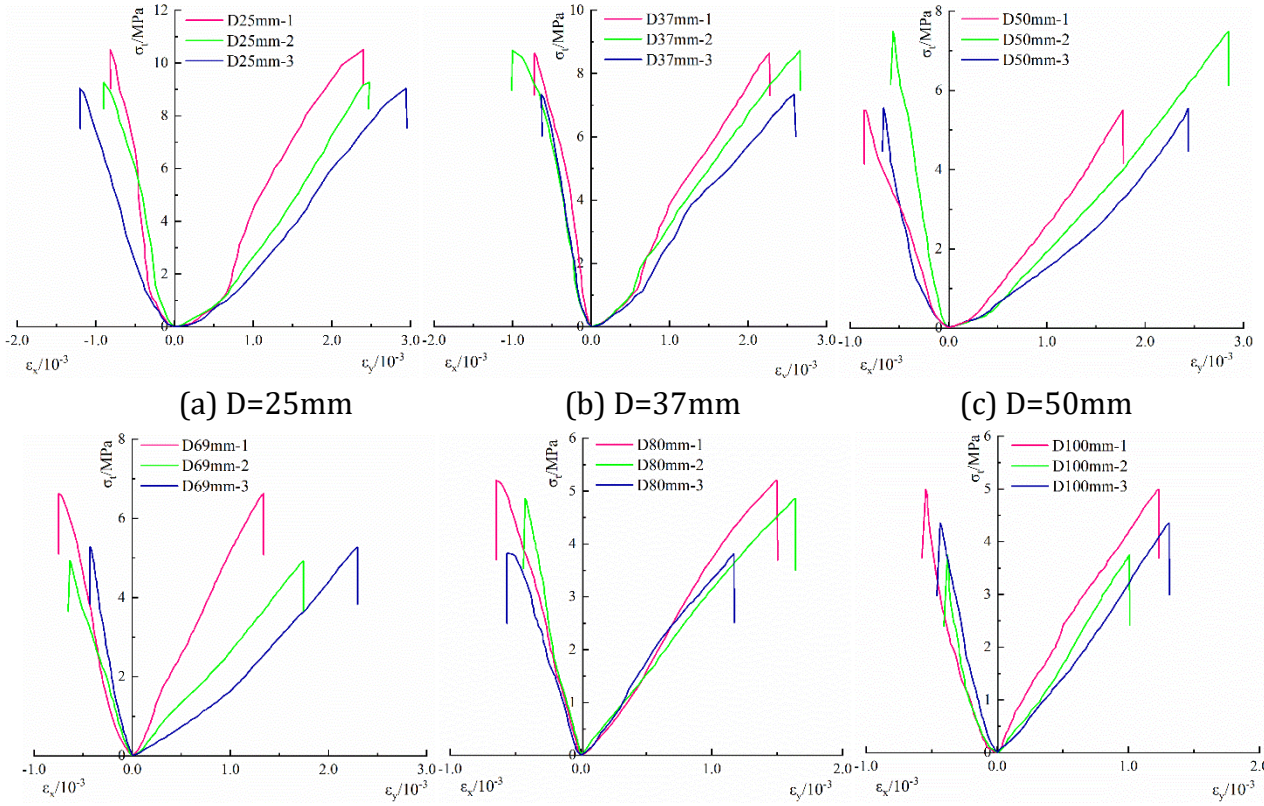


(a) D=25mm (b) D=37mm (c) D=50mm

(d) D=69mm (e) D=80mm (f) D=100mm

**Figure 1.** Different diameter sample stress- (tension) strain curve

According to Figure 3, at the diameters of 25,37,50,69, respectively, 80 and 100mm, the average tensile strength is 9.62,8.23,6.18,5.61,4.62,4.36MPa, the sample diameter is 25mm, and the 100mm is the smallest, and the average intensity value is 0.45 times of 25mm. In the process of increasing the sample diameter from 25mm to 100mm, the tensile strength of the sample was attenuated successively, with the average intensity attenuation value being

ISSN: 2710-0588

1.39,2.05,0.57,0.99,0.26MPa successively, and the attenuation amplitude was 14.4%, 24.9%, 9.2%, 17.6% and 5.9%. Therefore, it can be seen that when the disk thickness is certain, the diameter has a great influence on the development trend of the stress-strain curve and the peak value of the splitting strength. The main cause of this phenomenon is that the original defects number and scale of the rock material shows a certain relationship, the larger the size of the sample, the larger the number and scale of the deformation and damage of the larger defect size [14], and under the vertical load, sample end stress concentration, stress passed down along the load path, and the size of the larger sample by crack tip stress concentration, after reaching the crack stress, crack rapidly expansion, as the load continues to increase, crack through, forming macroscopic crack, instability damage.

Figure 4 shows the relationship between the split strength and the diameter of the deep gray sandstone samples. The scatter plot is drawn with the abscissa as the sample diameter and the ordinate as the peak tensile strength, and the average value of the split strength of different sizes is fitted. The fitted curve is shown in the figure below.

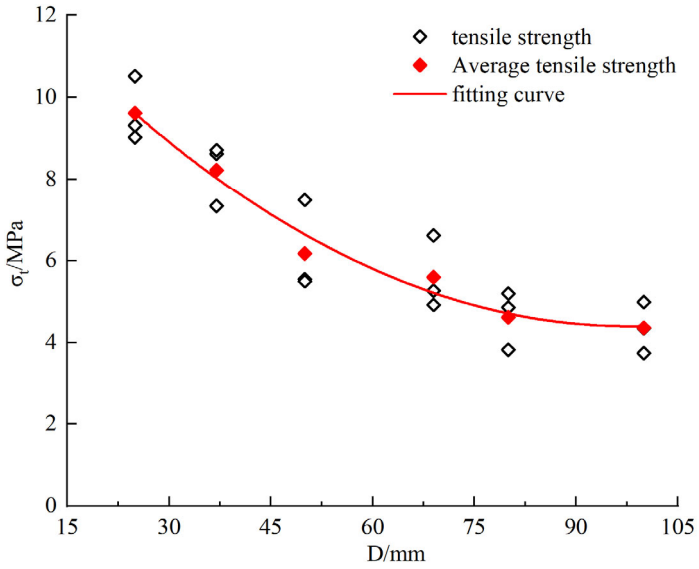


**Figure 2.** The peak split intensity fits with the diameter

## 3.3. Analysis of deformation characteristics

Under the action of the online load of the disk sample, the internal force is not uniform, which is subjected to the compression stress at the upper and lower edges of the disk adjacent to the loading plate, and the rest of the loading path is subjected to tensile stress. To better analyze the relationship between disc diameter and strain, tensile strain and compression strain was recorded during the test process, and the scatter plot was drawn as shown in Figure 5.

As can be seen from Figure 5, under the same thickness, the disk size has a great influence on the peak pressure (pull) strain of the sample, and with the increase of the size, the peak pressure (pull) strain generally shows a stable downward trend. As shown in Table 1, the mean peak tensile strain corresponding to the increase of the disk size from 25mm to 100mm is-$0.97\times10^{-3}$, $-0.78\times10^{-3}$, $-0.70\times10^{-3,}$ $-0.60\times10^{-3}$, $-0.55\times10^{-3}$, $-0.45\times10^{-3}$, respectively. The peak pressure strain was $2.60\times10^{-3}$,$2.50\times10^{-3}$,$2.34\times10^{-3}$,$1.79\times10^{-3}$,$1.43\times10^{-3}$,and $1.18\times10^{-3}$, respectively. The diameter of 50mm to 80mm corresponds to the peak pressure strain of $0.55\times10^{-3}$ and $0.36\times10^{-3}$, respectively, and the attenuation was 23.5% and 20.1%. As the size increased, the sample showed more obvious fragility. As can be seen from figure 5, the peak pressure strain of the same size sample is larger than the peak tensile strain, the ratio of the two in 2~4 times range, this result, mainly due to the compressive strength of the rock is greater

ISSN: 2710-0588

than the tensile strength, and the compressive strain in the micro crack compaction stage change is larger, and the tensile area under the tensile stress directly into the elastic stage until the peak damage. As can be seen from Figure 5, except that the disc diameter is 50mm, the other strain numerical error is within the reasonable range.

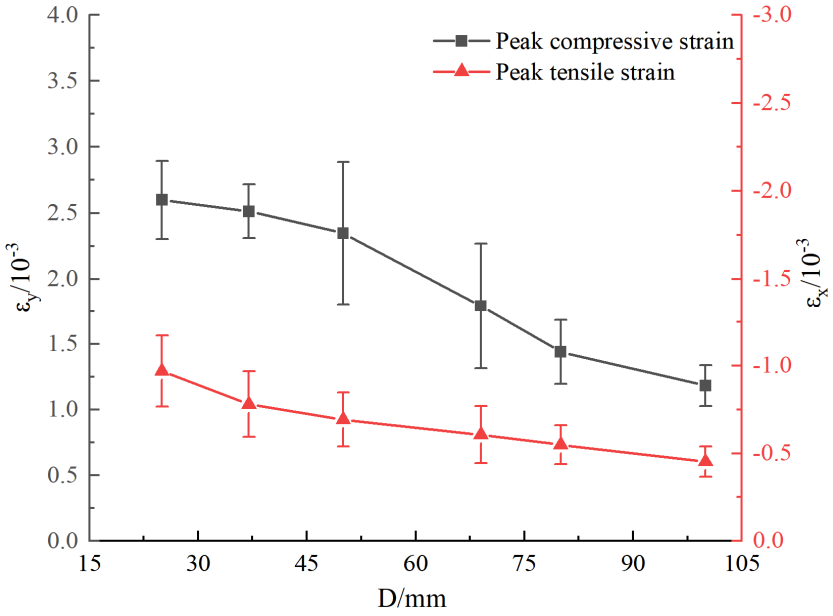


**Figure 3.** Relationship between disc sample diameter and peak split pressure (pull) strain

## 4. AE Features

### 4.1. AE ringing counting characteristics

According to the change of acoustic emission signal, the evolution law of crack and expansion of rock can be quantitatively described. In order to study the damage evolution characteristics of different size sandstone samples, the stress-time curve and the corresponding acoustic emission signal obtained by the 50mm diameter disk split test for example (as shown in figure 6), the whole process of rock damage is divided into four stages: (1) microcrack compaction stage (A-B), the initial loading stress increase faster, the acoustic emission signal appears less, this stage is the energy accumulation stage. Due to the insufficient load, the cumulative AE count curve is a straight line; (2) New crack generation and expansion stage (B-C). With the increase of load, energy accumulates, original cracks expand, new cracks arise, and a small amount of AE signals appear, and the increase of stress and cumulative AE signals is stable.(3) In the crack sharp expansion stage (C-D), the stress value reaches 80% of the peak stress, there are obvious acoustic emission signal fluctuations, the crack occurs through and further expanded, but the macroscopic rupture surface has not yet formed.(4) In the destruction stage (D-E), the stress value exceeds 95% of the peak stress, the acoustic emission signal increases sharply, the cumulative increase of ringing count is more than 3 times that before the D point, then the stress reaches the peak, the tensile stress near the loading path, the main crack develops rapidly, and the specimen is destroyed.

ISSN: 2710-0588

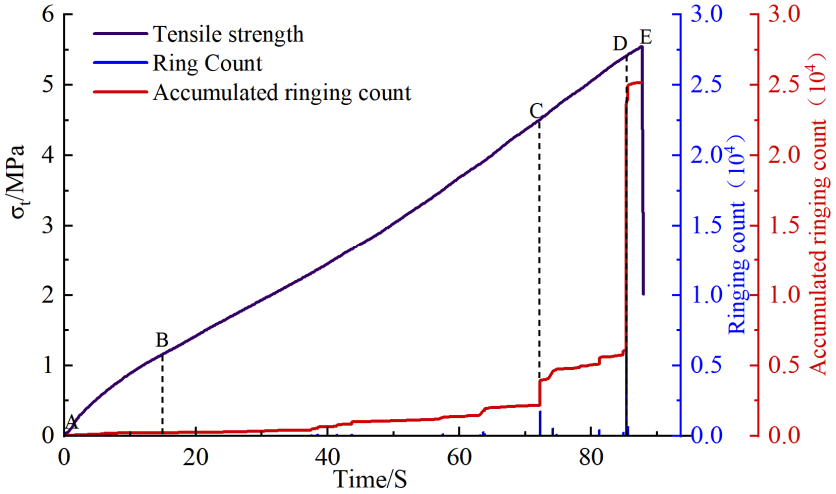


**Figure 4.** Curve of stress and ringing count over time

AE energy and acoustic emission ringing counting are usually used to reflect the rock internal fracture formation, development of energy consumption and the degree of internal damage. Figure 7 shows the relationship curve of AE ringing count, accumulated energy and stress over time during the splitting of samples of different sizes. The acoustic emission signal of one representative sample from each group of different sizes was selected for analysis. As can be seen from Figure 7, in the early stage of loading, the stress of each size sample increases rapidly, and the acoustic emission activity rarely appears. The sample is in the compaction stage, and almost no new cracks are produced inside. With the increase of stress, the AE signal will fluctuate several times, but the AE ringing count and accumulated energy are always in the low stage until the stress value inside the sample approaches the peak stress, the macroscopic crack appears on the surface of the sample, and the AE signal increases sharply, and then destroys. However, there are some samples with obvious acoustic emission signals before destruction. Analysis of the reasons shows that there is an initial defect along the loading path of the sample. Under the action of force, the micro-cracks at the defect expand, resulting in damage or damage in this area, but the overall stability of the sample is not affected and can continue to be carried. As can be seen from Figure 7, the small size sample showed obvious ringing count and energy changes during the loading process, while the large size sample only showed a surge of ringing count and large energy fluctuations at the moment of destruction.

The acoustic emission signal characteristics shown by different diameters are basically consistent with the damage mode. When the size is small, the damage type is complex, and the end of the sample is locally damaged to different degrees, which leads to the relative dispersion of the acoustic emission signal. For large samples, the rupture surface of the sample is mainly produced in the loading path, which is caused by the penetration of a single split surface, and the acoustic emission signal is relatively concentrated.

## 4.2. Analysis of the characteristics of the acoustic emission b-values

As a representation of the relationship between earthquake magnitude and frequency, *b* value was proposed by B.Gutenberg and C.F.Richter in 1941, and was later applied to the study of acoustic emission technology of rocks. It reflects the change of the internal crack scale of the rock during the loading process, and is of great significance to analyze the initiation, expansion and penetration of the internal crack of the sample. The calculation formula of *b* value is shown in equation (2) [15]:

ISSN: 2710-0588

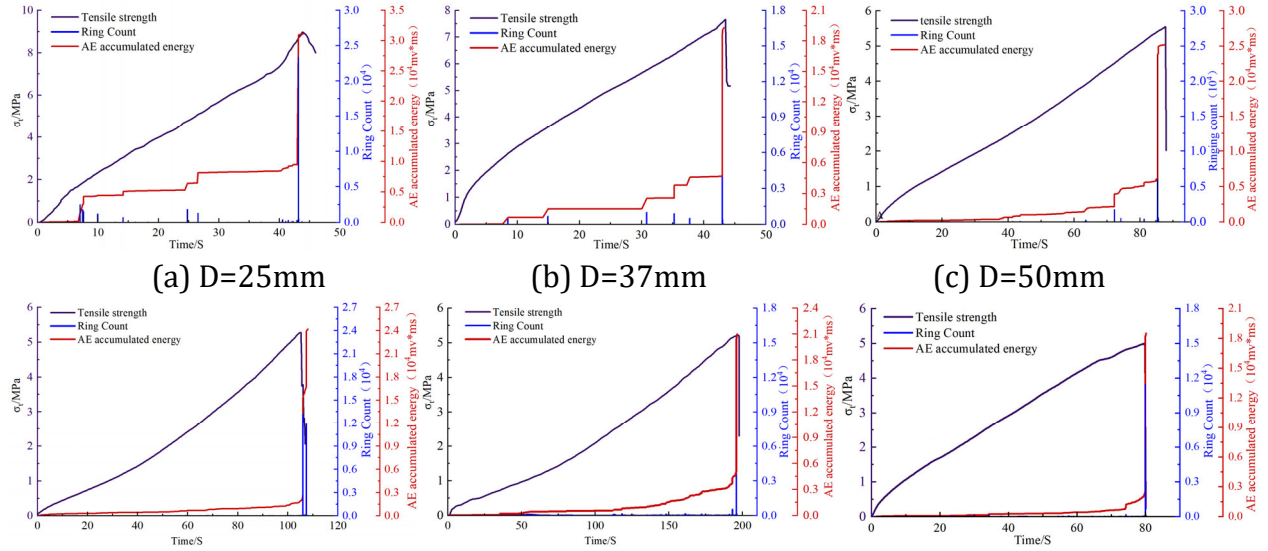


(a) D=25mm (b) D=37mm (c) D=50mm

(d) D=69mm (e) D=80mm (f) D=100mm

**Figure 5.** Stress, AE ringing count, and AE accumulated energy change curve over time

$$\lg N = a - bM \tag{2}$$

In formula:$N$ is the number of earthquakes in the range of magnitude interval, taking the number of impacts greater than the AE amplitude; $a$ is constant; $M$ is the AE magnitude, $M=a/20$, A is the AE amplitude in db. In this paper, the least squares method is used to calculate the $b$ value. For the short time from the initial loading to the sample destruction, 100 AE amplitude data are taken as the sampling window, the sliding window is 10, and the magnitude interval $\Delta M$ is 0.1 db.

The AE $b$-value curve shows the stability of the microcrack, and the pattern is flat. The decrease of $b$ value (increase) means that the internal fissure of the specimen develops to a large scale (small scale). Figure 8 shows the stress-time-$b$ value curve during loading.

Figure 8 (a) shows the stress-time-b value curve of the 25mm diameter sample. As can be seen from the figure, in the early stage of loading of the sample, the stress increases rapidly, and the AE $b$ value is sparse, and at this time, the internal fissure of the sample is in the compaction stage. When the stress reaches $0.18\sigma_t$, the $b$ value shows a small decrease, which means a small amount of large-scale rupture inside the sample, which corresponds to the obvious ringing count in Figure 7 (a) and the energy burst. When the stress reached $0.39\sigma_t$, the $b$ value maintained a short time steady change, indicating that the fissure inside the specimen developed and stable during this period. When the stress value is in the range of $0.49\sigma_t \sim 0.85\sigma_t$, the $b$ value is always in a violent oscillatory state, and the adjacent $b$ value changes in the range of 0.4～1.0, indicating that the fissure inside the sample is in an unstable extended state, and the large and small scale rupture occurs alternately. When the stress reaches $0.91\sigma_t$, the stress increases rapidly and the $b$ value decreases, which means that the sample has large scale rupture and instability damage occurs at any time. It should be noted that, due to the sliding friction of the macroscopic rupture surface of the sample, the stress reaches the extreme value, and the $b$ value rises slightly and then drops immediately.

The 50mm diameter specimens are described in Figure 8 (b). As can be seen from the figure, when the stress is within the range of $0.33\sigma_t \sim 0.52\sigma_t$, the b value trend is stable, the cracks are in the stable expansion stage, and small scale cracks are constantly produced. When the stress reached $0.74\sigma_t$, the $b$ value rose from 0.8 to 1.4, and in the next 10 seconds, the b value

ISSN: 2710-0588

decreased from 1.43 to 0.39, indicating that the specimen entered the unstable rupture phase, in which large-scale cracks were generated. At 77 seconds, the corresponding stress value is $0.94\sigma_t$, and the value of *b* has experienced 4 sudden changes, the maximum range of change is 1.57, and the minimum is 0.15, indicating that when the stress reaches the peak stress, there are many large scale cracks, accompanied by a small number of small scale rupture.

The 100mm diameter sample is described in Figure 8 (c). It can be seen from the figure that the stress appears less frequently in the range of $0\sim0.83\sigma_t$, and the generation of cracks in this process is mainly dominated by small rupture, and the degree of rupture is stable. With increasing load, the *b* value rises sharply from 1.1 to 1.7 and fluctuates around 1.6, which is dominated by small ruptures. When the stress value reached $0.86\sigma_t$, the trend of the *b*-value fluctuated, which meant the unstable expansion of the crack inside the specimen. When the stress value reaches $0.95\sigma_t$, the *b* value drops from 1.8 to 0.8, which corresponds to the large-scale rupture inside the sample, which also means that the instability destruction occurs at any time. The stress value is from $0.95\sigma_t$ to the peak stress stage, and the sample maintains the original stability, but from the trend of *b* value, we can see that the internal rupture is rapidly to different degrees, mainly large scale rupture at the moment.

In conclusion, the stress values corresponding to the instability expansion of the internal fissure in the diameter of 25mm, 50mm and 100mm samples are $0.49\sigma_t$, $0.74\sigma_t$ and $0.86\sigma_t$, respectively. The larger the size of the sample, the smoother the trend of AE *b* value, the greater the change of *b* value caused by the internal crack of the sample entering the instability expansion stage, and the more severe the damage of entering the instability stage.

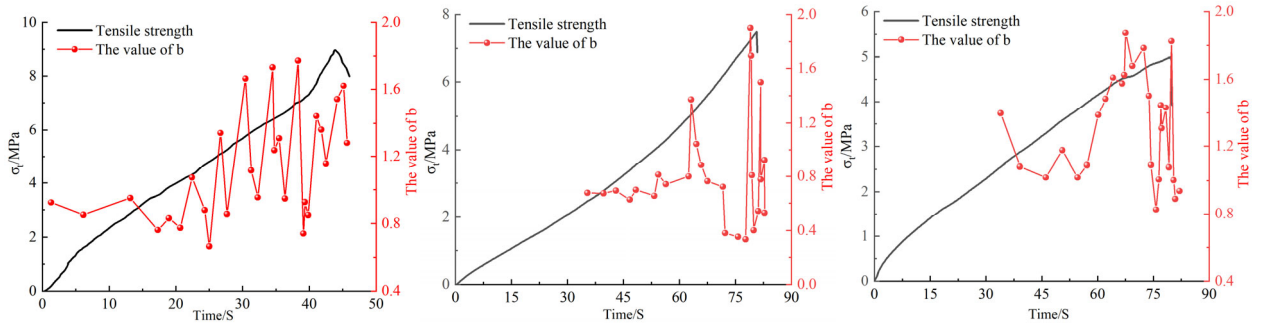


(a) D=25mm ( b) D=50mm (c) D=100mm

**Figure 6.** Stress-time-*b* value curve

## 4.3. Analysis of damage destruction characteristics based on acoustic emission signals

According to the difference of Aemission waveform. It is generally believed that the formation of tension cracks corresponds to higher *AF* and lower *RA* values, and shear cracks correspond to lower *AF* and higher *RA* values. Therefore, the failure characteristics of internal rock cracks can be analyzed by *RA* (reflecting the rising Angle) and *AF* (average frequency). Ohstu et al. [16] gives the following calculation formula as follows:

$$RA = \frac{AERiseTime}{AEAmplitude} = \frac{A_{RT}}{A_A} \tag{3}$$

$$AF = \frac{AECount}{AEDuration} = \frac{A_C}{A_D} \tag{4}$$

ISSN: 2710-0588

In formula:$A_{RT}$ is the acoustic emission rise time, $A_A$ is the acoustic emission amplitude,$A_C$ is the acoustic emission bell count, and $A_D$ is the duration of the acoustic emission.

Literature [17] believes that the diagonal of *RA-AF* distribution map can be used as the dividing line of pull-shear microcracks, with the tensile microcracks above the diagonal, and the shear microcracks below the diagonal. The acoustic emission data were processed according to the above formula. In order to directly reflect the type of microcrack, the *RA-AF* density map of 25mm, 50mm and 100mm was drawn with *AF* (MHz) as the X-axis and *RA* (ms / V) as the Y-axis, as shown in Figure 9. In the figure, the density of the orange yellow area is the largest, and the density of the blue area is 0. As can be seen from the figure, the cracks generated by the splitting test are mainly tensile micro-cracks. With the increase of the sample size, the core density area gradually increases, and the total amount of cracks increases, especially the tensile micro-cracks gradually increases. The size is small, the crack development is slow, corresponding to the total amount of cracks produced is less. When the size is large, the crack expansion is complete, and the tension damage is obvious.

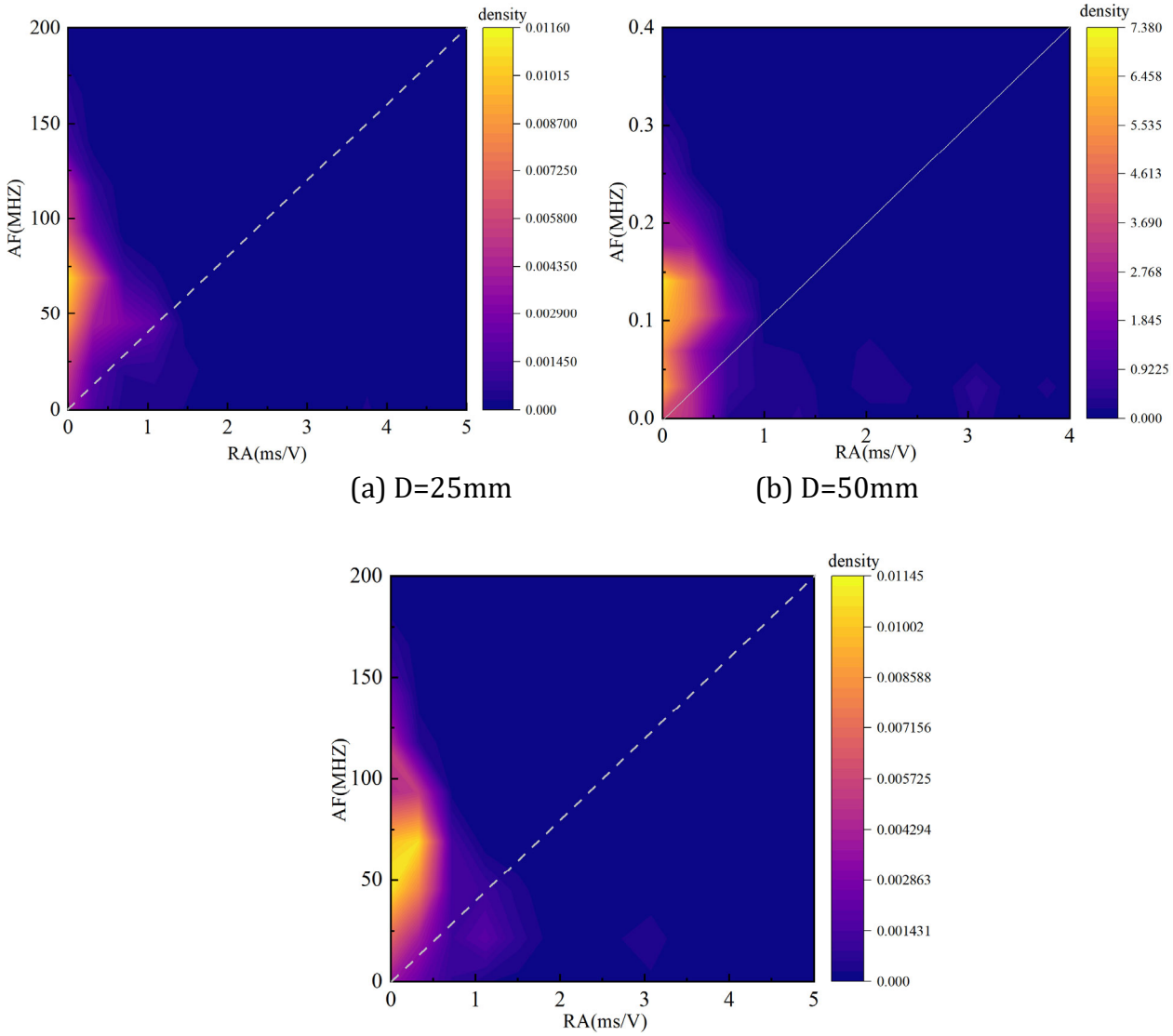


**Figure 7.** The density profiles of RA-AF with 25mm, 50mm, and 100mm

ISSN: 2710-0588

To further reflect the correlation pattern of the type of microcracks produced during the test, the proportion of shear and tensile microcracks was described by drawing the bar graph. The hear and tensile microcracks generated during splitting are shown in Figure 10. It can be seen from the figure that the tensile microcracks occupy a large proportion, so it can be seen that the crack formation type in the disk splitting process is mainly tensile cracks. As the diameter of the disc increases, there are fewer shear micro-cracks. The percentage of tensile microcracks of 25mm was 68.3%, and the percentage of 100mm increased to 88.1%, an increase of 29.3%, indicating that the number of tensile microcracks increased with the increase of diameter, with obvious size effect.

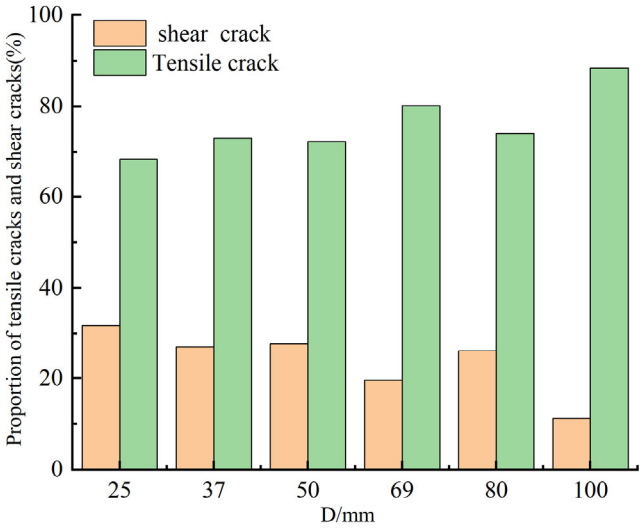


**Figure 8**. Effect of size on tensile and shear micro-cracks

## 5. Conclusion

(1) For samples with diameter between 25mm-100mm, the size is negatively correlated with peak strength and peak strain, and the ratio of peak pressure strain to peak tensile strain of the same size is 2 to 4 times. With increasing size, the specimens showed a more pronounced fragility.

(2) The diameter samples of 25mm and 37mm showed obvious ringing counts several times before destruction, while the ringing counts of 50mm-100mm samples increased slowly during the loading process, while the Aemission signal activity of disk samples of different sizes was concentrated in the moment of destruction.

(3) According to the acoustic emission data, the change curve of b value of the sample during the loading process is drawn, and it is concluded that with the increase of the sample size, the larger the stress value, the more obvious the curve oscillation, the larger the size of the sample, the more intense the rupture degree of the instability stage.

(4) The cracks generated in the sample of each size are mainly tensile micro-cracks. With increasing sample size.

## References

[1] PING Qi, ZHANG Hao, SU Haipeng.Study on dynamic compression mechanical properties of limestone with different lengths [J]. Chinese Journal of Rock Mechanics and Engineering, 2018, 37(S2): 3891-3897.

ISSN: 2710-0588

[2] ZHANG Sheng, WANG Zheng, ZHANG Xulong,et al.Rock dynamic mechanical properties and dynamic stress balance of sandstone specimens with different sizes[J] Explosion and Shock Waves, 2022, 42(10): 22-38.

[3] ZHANG Sheng, YU Bingxin, WANG Feng, et al. Experimental study on dynamic fracture characteristics of different sizes of rock specimens with a crack [J] Journal of Mining & Safety Engineering, 2021, 38(05): 1045-1054.

[4] ZHANG Sheng, AN Dingchao, ZHANG Xulong, et al. Research on the size effect of rock dynamic fracture toughness considering the influence of space-time domain[J].Chinese Journal ofRock Mechanics and Engineering, 2022, 41(10): 1981-1992.

[5] ZHAO Guangming, LIU Zhixi, MENG Xiangrui, et al.Energy accumulation and dissipation testand analysis method of height-diameter ratio sandstone[J].Journal of China Coal Society,2022,47(03): 1110-1121.

[6] ZHAO Guangming, ZHOU Jun, MENG Xiangrui, et al.Dynamic impact compression characteristics of granite rocks with different length-diameter ratios[J].Chinese Journal of Rock Mechanics and Engineering, 2021, 40(07): 1392-1401.

[7] SUN Hao, SU Nan, JIN Aibing, et al.Effects of temperature on Brazilian splitting characteristics of sandstone with different sizes[J].Chinese Journal of Engineering, 2022, 44(01): 26-38.

[8] ZHAO Fei, WANG Hongjian, HE Manchao, et al.Acoustic emission characteristics of granite specimens with different heights in rockburst tests[J].Rock and Soil Mechanics ,2019,40 (01):135-146.

[9] LIU Gang, XIAO Fukun, QIN Tao. Rock mechanics characteristics and acoustic emission ruleunder small-size effect[J].Chinese Journal of Rock Mechanics and Engineering, 2018, 37(S2):3905-3917.

[10] LIU Hui, LIN Jianghao, YANG Gengshe, et al.Acoustic emission test on tensile damage characteristics of sandstone under freeze-thaw cycle[J].Journal of Mining & Safety Engineering, 2021, 38(04): 830-839.

[11] WANG Yunfei, LIU Xiao, WANG Liping, et al.Coupling effect of loading rate and saturated water on mechanical behavior and micro damage property of sandstone[J].Journal of Mining& Safety Engineering, 2022, 39(02): 421-428.

[12] DONG Jinpeng, YANG Shengqi, LI Bin, et al.Experimental study on the tensile strength of rock-like materials containing two pre-existing coplanar fissures[J].Engineering Mechanics, 2020, 37(03): 188-201.

[13] WU Faquan, QIAO Lei, GUAN Shenggong, et al.Uniaxial compression test study on size effect of small size rock samples[J].Chinese Journal of Rock Mechanics and Engineering, 2021, 40(05): 865-873.

[14] SUN Ruda, ZHANG Chuanjiu, LI Hongping, et al.Study on influence of multi-scale effect on coal bursting liability[J].Coal Science and Technology, 2022, 50(S2): 170-179.

[15] LIU Xiling,LIU Zhou,LI Xibing, et al.Acoustic emission b-values of limestone under uniaxial compression andBrazilian splitting loads[J].Rock and Soil Mechanics , 2019,40(S1):267-274.

[16] OHTSU M,ISODA T,TOMODA.Y. Acoustic emission techniques standardized for concrete structures [J]. Journal of Acoustic Emission,2007,25:21-32.

[17] Bai Jinwen, Yang Xinyu, Shi Xudong, et al. Effect of FRP wrapping on the splitting failure characteristics of coal-filled structures[J]. Chinese Journal of Rock Mechanics and Engineering,2023, 42 (S1): 3541-3557.